Geochemical characteristics of different iron ore types from the Southern Tomašica deposit, Ljubija, NW Bosnia

Vesnica Garašić and Ivan Jurković

Faculty of Mining, Geology and Petroleum Engineering, University of Zagreb, Pierottijeva 6, HR-10000, Croatia; (vesnica.garasic@rgn.hr)

Geologia Croatica

ABSTRACT

Pulverized limonite ore from a Pleistocene–Quaternary lake deposit and compact limonite ore from the Olistostrome member of the Javorik flysch formation, in the Southern Tomašica iron ore deposit, were investigated and compared with different types of siderite and ankerite, limestone and carbonate shale from the same location in order to determine their possible protolith. Two limonite types display a notably distinct REE pattern, REE fractionations, Eu anomalies and other trace element and main oxide content. The REE pattern of compact limonite is characterized by relatively low light ($(La/Sm)_N = 2.87$), heavy ($(Gd/Yb)_N = 0.98$) and total ($(La/Yb)_N = 3.19$) REE fractionations, a strong positive Eu anomaly ($Eu/Eu^* = 2.11$) and weakly expressed negative Ce anomaly ($Ce/Ce^* = 0.82$). The compact limonite and siderite REE patterns almost overlap suggesting a common REE source. The same is valid for their Zr/TiO_2 ratios (0.040 in the compact limonite, 0.033–0.053 in the siderites). Pulverized limonite shows remarkably different REE patterns and the highest REE concentrations, (up to 6 to 13 times higher relatively to the other samples). Its REE fractionation pattern ($(La/Sm)_N = 3.68$, $(Gd/Yb)_N = 1.58$, $(La/Yb)_N = 9.41$, $Eu/Eu^* = 1.10$ and $Ce/Ce^*_N = 0.81$) is very similar to those in the carbonate shale, identifying it as the possible protolith of pulverized limonite. The same is valid for the Zr/TiO_2 ratios (0.025 in pulverized limonite and 0.017 in carbonate shale). The REE pattern of fine grained ankerite ($(La/Yb)_N = 2.15$, $Eu/Eu^* = 1.95$, $Ce/Ce^* = 0.78$) and its Zr/TiO_2 ratio (0.030) are similar to those in siderite, and could, assuming extensive contamination of pulverized limonite, also represent its protolith. However, the REE patterns of coarse grained ankerite exhibit remarkable depletion of LREE over HREE and a strong reverse LREE pattern ($(La/Yb)_N = 0.05–0.20$, $(La/Sm)_N = 0.04–0.10$, $(Gd/Yb)_N = 1.77–1.91$). They have (similar to the other studied samples), a positive Eu anomaly ($Eu/Eu^* = 2.16–2.75$) and negative Ce anomaly ($Ce/Ce^* = 0.32–0.83$). Their Zr/TiO_2 ratio (0.004–0.010) excludes coarse grained ankerite as the possible protolith of pulverized limonite.

Keywords: compact limonite, pulverized limonite, REE pattern, siderite, ankerite, Southern Tomašica

1. INTRODUCTION

Southern Tomašica is one of the four opencast mines (Adamuša, Vidrenjak, Tomašica and Omarska) in the Ljubija iron ore field, situated approximately 200 km northwest of Sarajevo, in Bosnia and Herzegovina. Southern Tomašica is a large deposit of siderite, ankerite, compact limonite and pulverized limonite laying 18 km southeast of Prijedor. It is located on the northern side of the mountain system of Ljepovica (+678 m) and Mačkovac (+474 m) and bordered to the west by the Velika Gradina plateau (Fig. 1).
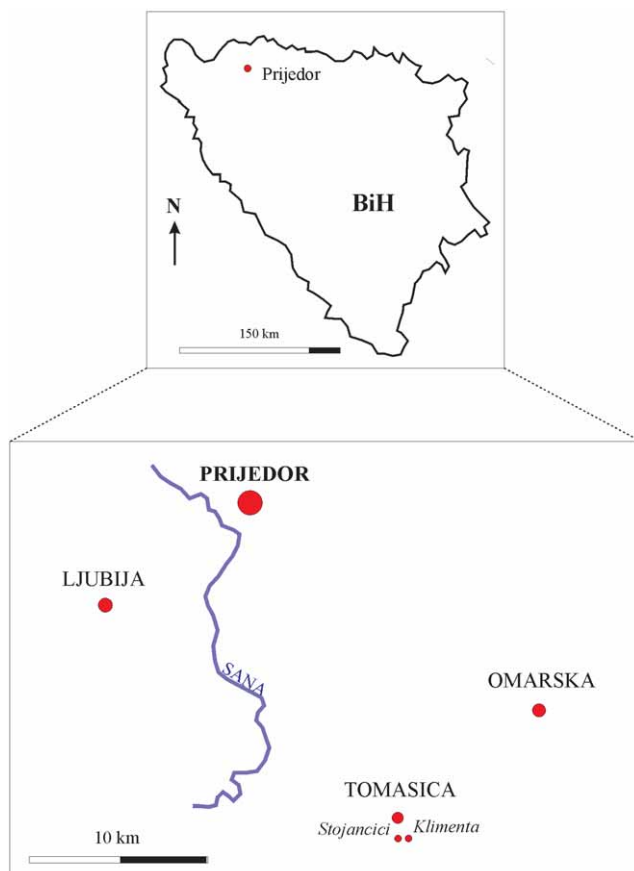
Figure 1: The location of the studied area.

The origin and time of formation of the iron deposits in the Ljubija iron ore field are matters of considerable debate. GRUBIĆ & PROTIĆ (2003) clearly distinguishes an older siderite-limonite formation and a younger ankerite-limonite formation. According to them, siderite occurring as lenses and alternating with black argillaceous schist in the siderite-limonite formation, originated as primary non-magmatic hydrothermal marine sediment in the Lower to Middle Carboniferous. The first evidence of the synsedimentary origin of this siderite was provided by JURKOVIĆ (1961). JURIĆ (1971) shared the same opinion. GRUBIĆ & PROTIĆ (2003) discovered fissures filled with iron and manganese minerals in Upper Flysch, Permian and Werfenian sediments of Southern Tomašica. Therefore they concluded that ankerite replacing carbonate rock fragments in flysch and small siderite bodies, associated with the carbonate olistoliths in the Olistostrome Member of the Javorik flysch formation, was precipitated from hydrothermal solutions partly associated with porphyrite volcanism in the Middle Triassic. STRMIĆ PALINKAŠ et al. (2009) regarded iron deposits within the Ljubija field as stratabound Fe carbonate ore bodies, hosted by marine limestones, and as siderite-sulfide veins within Carboniferous shales. They concluded that Fe mineralization occured through hydrothermal-metasomatic processes in the Permian, in accordance with the earlier opinions of PALINKAŠ (1988, 1990), PALINKAŠ et al. (2003) and BOROJEVIĆ ŠOŠTARIĆ (2004).

Later in geological time, siderite and ankerite ore bodies were partly oxidized and hydrated to various types of limonite ore (JURKOVIĆ, 1961; JURIĆ, 1971; GRUBIĆ & PROTIĆ, 2003). Although the mineralogy and major element chemistry of different limonite ore types from the Southern Tomašica mine have been described earlier (JURKOVIĆ, 1961; ŠARAC, 1981), their REE patterns are still unknown.

The aims of this study are to present the results of more detailed geochemical analyses for two different limonite ore types and compare them with the REE distribution patterns of ankerite, siderite, host limestone and carbonate shale, from the Olistostrome Member of the Javorik flysch formation, in order to establish their possible genetic relationships.

2. GEOLOGICAL SETTING

The area of Southern Tomašica consists mainly of sedimentary rocks of Carboniferous, Permian, Werfenian and Quaternary age (Fig. 2), which were metamorphosed, folded and faulted during the Variscan and Alpine orogenies (Fig. 3).

Carboniferous rocks belong to the Javorik flysch formation, and the Permian rocks to the Tomašica clastite formation. The most detailed stratigraphic column of this area was drawn by GRUBIĆ et al. (2000) and GRUBIĆ & PROTIĆ (2003) on the basis of field work (M 1:1000) and core descriptions from 520 wells (Fig. 4). According to GRUBIĆ & PROTIĆ (2003) the Javorik flysch formation consists of six members. The oldest member is the Lower Flysch characterized by dark green argillaceous schists, alternating with medium-grained sandstone. It is followed by the Siderite-Limonite member which is up to 30 m thick, becoming thinner at the margins. This member contains massive siderite alternating with black argillaceous schist. Siderite is partly transformed to limonite. The Wild Flysch member, (<50 m thick), overlies the Siderite-Limonite member. It consists of two black argillaceous phyllite packets and one sandstone packet. It exhibits characteristic spheroidal and tube-like olistolithes at the decimetre-level on the surface. The Wild Flysch member is overlain by the Middle Flysch member which is about 60 m in thickness, consisting of alternations of argillaceous schist, (subflysch), sandstone (argillaceous euflysch) and sandstone (coarse flysch). It contains variably sized olistostrome lenses with mineralized limestone fragments, sandstone banks and rare microconglomeratic sequences. The Middle Flysch member is overlain by an Olistostrome member, which is 800 m long and 50 to 150 m wide, consisting of flysch matrix in which carbonate olistolithe fragments, blocks and their mineralized parts are embedded. The Flysch groundmass of the Olistostrome member is mainly sandstone flysch, the lower and upper parts of which are composed of grey and dark grey medium-grained sandstones, and black laminated siltstones, respectively. Carbonate fragments and blocks of the Olistostrome member include black micrites, dark grey organogenic sparites (rich in fossils), dolomite limestones, dolomites, ankeritic limestone and ankerite. The occurrence of pulverized limonite, which in larger blocks represents the transition from ankerite and
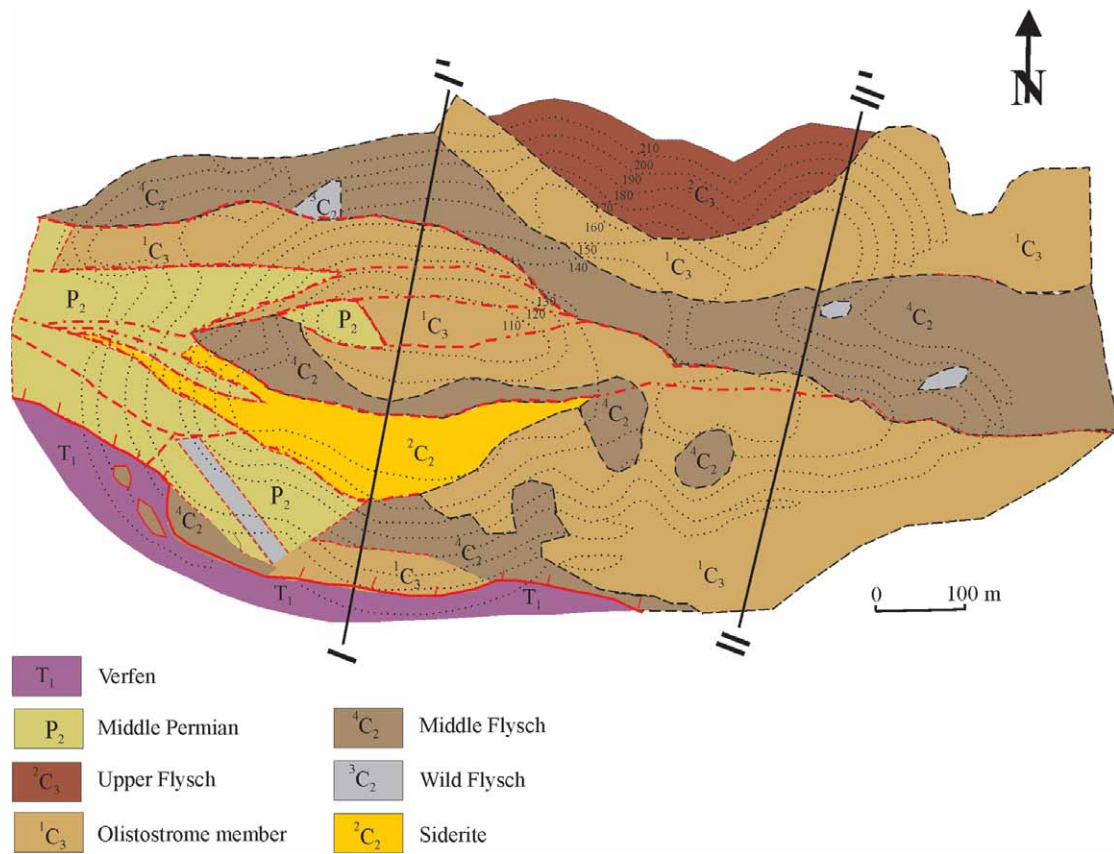
Garašić and Jurković: Geochemical characteristics of different iron ore types from the Southern Tomašica deposit, Ljubija, NW Bosnia

257

Geologia Croatica

Figure 2: Geological units of the Tomašica area (GRUBIĆ & PROTIĆ, 2003).

dolomite limestones into fossiloferous limestones, is important. Typically, up to 3–4 m large isolated, spheroidal and irregular bodies of partly comb-textured ankerite and dolomite limestone, completely enclosed by pulverized limonite occur in this member. They appear in groups of several bodies in pulverized limonite profiles having a thickness of several tens of metres. In addition to this description of GRUBIĆ & PROTIĆ (2003), STRMIĆ PALINKAŠ et al. (2009) discovered in the Olistostrome member, dark massive siderite being locally weathered to porous, but compact limonite, while the present authors observed numerous dark limestones cut by veins of siderite, ankerite and calcite. In the
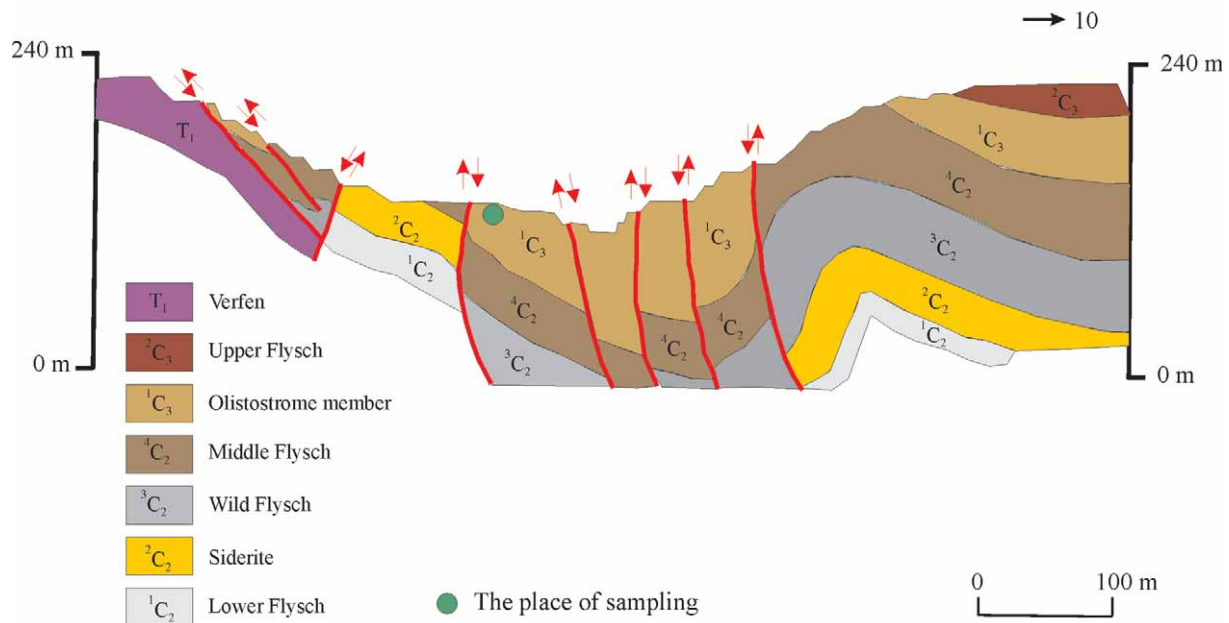

Figure 3: Geological profile I-I' (Fig. 2) of Southern Tomašica (GRUBIĆ & PROTIĆ, 2003). Sampling locations are marked.

flysch groundmass of the Olistostrome member, carbonate shale occurs as a small isolated body. According to GRUBIĆ & PROTIĆ (2003), the last and the youngest member of the Javorik formation is the Upper Flysch, being located on the northern side of the opencast. It is 700 m long, 140 m wide and 70 m thick. The lower part of this member is particularly black in colour, and mostly composed of sandstone-siltstone flysch. The black colour comes from Mn oxides and hydroxides, and is more weakly expressed in the upper part, where sequences are at the centimetre scale.

The Tomašica clastite formation is located on the western side of the opencast mine, in the area of Velika Gradina. GRUBIĆ & PROTIĆ (2003) recognized five members of this formation: a) Bobovica breccias, b) white sandstones, c) white and red sandstones, d) polygenous conglomerates and e) red sandstones and siltstones.

The southern part of the Southern Tomašica opencast mine consists of marls, marl limestone, siltstones, sandstones and breccia-like intercalations of Werfenian age, which reach a thickness of around 70 m.

According to JURIĆ (1967) and PODUBSKI (1969), the rocks of the Javorik formations are metamorphosed at the highest grade of the greenschists facies.
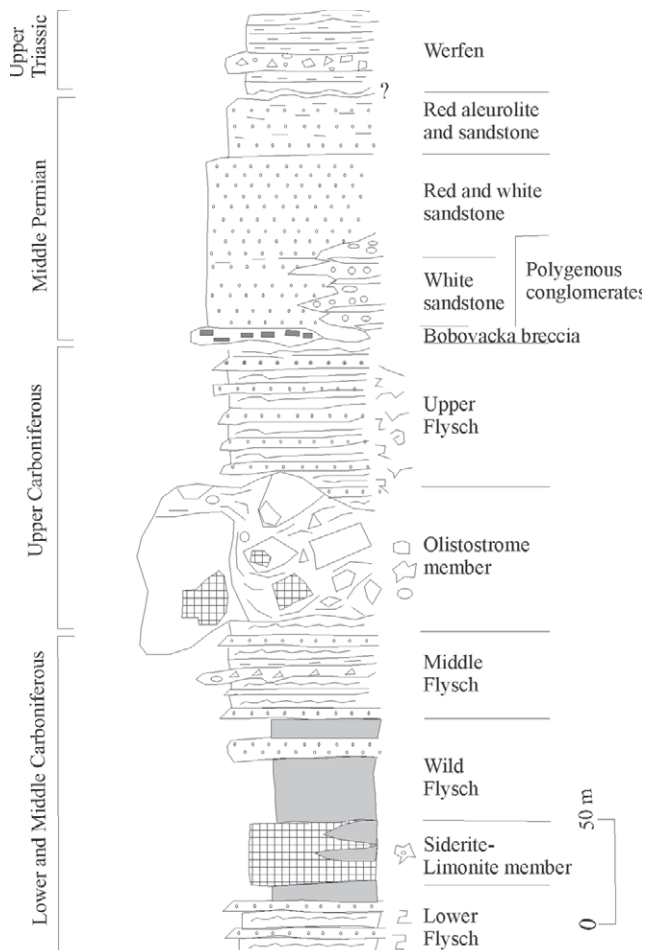

Figure 4: Stratigraphic column of Southern Tomašica (GRUBIĆ & PROTIĆ, 2003).

During the Tertiary, after uplift of the Upper Palaeozoic complex, the oxidation processes of primary iron ore (siderite, ankerite and ankeritized carbonate rocks) in Ljubija had begun and limonite gossans had been formed "in situ". According to JURKOVIĆ (1961), gossans developed by weathering of siderite were compact and stable, while those derived from massive ankerite were more mobile. Later, due to erosion, gravity, mechanical and chemical leaching and solution, different aureoles of secondary limonite ore were developed. In the Pliocene–Quaternary period remarkable part of this limonites were further transported by rain, river or wind, and redeposited in palaeovalleys, palaeobasins and lakes, partly as detrital limonite, partly as pulverized limonite or "brand" (termed by Jurković in publications). On this occasion limonites became more or less contaminated.

Reworked deposits of limonites and pulverized limonites in the Pliocene–Quaternary sequences of Jezero and Buvač near Omarska were described by JURIĆ (1969) and ŠARAC-VITALJIĆ (1973), and those in the Blatnjak deposit by JURIĆ (1971).

The best description of reworked deposits of limonite and pulverized limonite in the area of Tomašica (Southern Tomašica, Northern Tomašica, Šiljezi, Stankovići, Dabića Brdo, Tevanovići, Bojići) was by CVIJIĆ (1986, 2001). The ore bodies are mainly characterized by lense-like or cone-like shapes, rarely irregular layers, reaching thicknesses of 10–30 m, locally up to 50 m, rarely more than this. The borders of ore bodies are not sharp.

3. PREVIOUS STUDIES OF LIMONITES IN TOMAŠICA

Laboratory and commercial studies by LOGOMERAC (1960) have shown that pulverized limonite is a suitable ore-grade raw material for sintering, pelletizing and bricketizing in the production of raw iron. The granulometric composition of pulverized limonite was characterized by 26.8 wt.% of particles finer than 60 μm, 46.8 wt.% of particles ranging between 60 and 100 μm, 16.3 wt.% of particles laying between 100 and 400 μm and 10.0 wt.% of particles from 400 to 1500 μm diameter. The specific and volume weights were 3.3 g/cm^3, and 1.38 g/cm^3, respectively. The LOI was equal to 8.15% and H_2O^- to 6.8%.

The first laboratory, physico-chemical and optical studies of limonite samples from the Southern Tomašica ore district (Točak, Gradina, Stojančići and Klimenta localities) were performed by JURKOVIĆ (1961). The XRD analyses of pulverized limonite (brand) from Stojančići show mostly the presence of micro-cryptocrystallized goethite (70 wt.%), and some amorphous clay, having no peaks on the Debye diagram. DTA has given endothermic effects, which were strong at +200°C (goethite) and 350°C (partly amorphous limonite) and weak at temperatures from +550°C to +650°C (clay). TGA shows weight loss of 8% in the range between +100°C and +400°C (goethite-limonite), and 4 % between +550°C and +650°C (illite clay). The results of XRD, DTA and TG analyses reveal that the brand consists of a mixture

Garašić and Jurković: Geochemical characteristics of different iron ore types from the Southern Tomašica deposit, Ljubija, NW Bosnia

259

Geologia Croatica

of cryptocrystalline and partly amorphous goethite and allophanoid amorphous clay (68.25 and 8.65 wt.% respectively). The studied sample was prepared in Plexiglas and investigated under reflected light microscopy (Fig. 5). Pulverized limonite (brand) consists of pizoliths having diameters in the range of 30 and 300 μm, on average between 100 and 200 μm. Pizoliths are spheroidal, rarely oval and consist of an intimate mixture of cryptocrystalline goethite and amorphous or cryptocrystalline clay masses. In reflected light they have considerably lower lustre than goethite, are isotropic, and in crossed polars show diffusely scattered brown inner reflections.

ŠARAC (1981) analyzed pulverised limonite samples, discovering a very high content of SiO_2 (15.56%) and Al_2O_3 (3.40%) compared to compact limonite.

Studies in the Boris Kidrič Institute in Ljubljana and in Firma Bayer have shown that ore deposits of pulverised limonite in Tomašica represent a natural mineral pigment with a high content of natural chromofore (up to 80 %) which is applicable to the colour and varnish industry and in the industry of anticorrosive coating and coloured building materials. On the basis of these studies, a natural pigments factory was built in Tomašica using pulverised limonite raw material from the Southern Tomašica deposit and the Blatnjak deposit.

Detailed petrological characteristics of compact limonite have been described by JURKOVIĆ (1961). Using XRD analyses, he identified goethite as the main mineral intimately intergrown with illite which has sheets up to 10, and rarely up to 30 μm or more and with quartz crystals, occurring in bipyramidal prisms, with diameters in the ran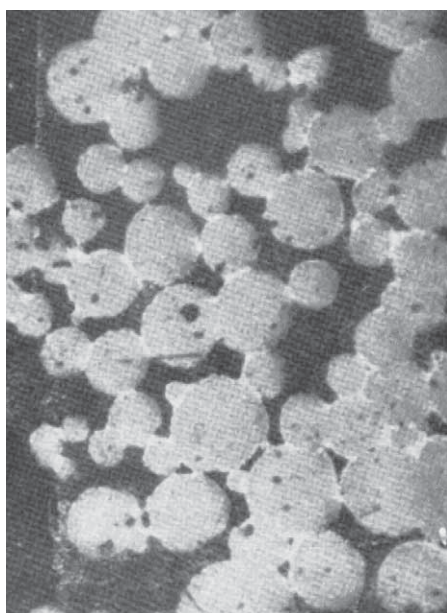ge between 30 and 300 μm, or in alotriomorphic masses. There are oxidized pyrite relics and minor lepidocrocite in massive goethite. Additionally, fine microscopic tiny veinlets of cryptocrystalline pyrolusite and microcrystalline pyrolusite in pores are also present in goethite. Cryptocrystalline or fibrous psilomelane also occur replacing goethite or being transformed into pyrolusite. The manganese minerals were most likely formed as a weathering product of siderite, which contains up to 2.55 wt.% of MnO. Elemental silver was observed in the goethite pores. Mineral intergrowths are frequent and fine-grained, or rare and coarse-grained.

3.1. Samples and analytical methods

All samples were collected within the Olistostrome member of the Javorik flysch formation excluding pulverized limonite (TBRA) which was found on an ancient mine heap at Stojančići representing relics of one Pleistocene–Quaternary lake limonite deposit.

Levels of the quarry containing the Siderite-limonite member have been submerged some years ago since mining operations ceased and it was impossible to collect samples from this part of the Javorik flysch formation.

Ten representative samples from the Southern Tomašica opencast mine and one from the Adamuša opencast mine have been studied in detail: compact limonite (TLIM) representing gossan formed in situ on siderite, pulverized limonite or "brand" (TBRA), limestone (TVAP1), carbonate shale (TVAP2), white-gray coloured ankerite (TMIX), white coarse grained ankerite (TANK, TANMIC), dark fine grained ankerite (TANK1), reddish coarse grained siderite (TCOR), dark fine-grained siderite (TMIC) and yellow coarse grained siderite (AD-2).

The sample of compact limonite (TLIM) represents a gossan formed "in situ" on siderite. It occurs in the form of black and shiny, kidney shaped concretions, and glassy needles (Fig. 6). Microscopic investigations show that the concretions have an internal radiating structure (Fig. 7) and the main mineral is goethite. Other minerals in the paragenesis are quartz, clay minerals and muscovite. This is in accord-

Figure 5: Spheroidal pizoliths consist of a mixture of cryptocrystalline goethite and amorphous or cryptocrystalline clay. White thin intergranular films of crypto- to microcrystalline goethite surround the pizolites. The black area is a hole. Magnification: x55 (after JURKOVIĆ, 1961).

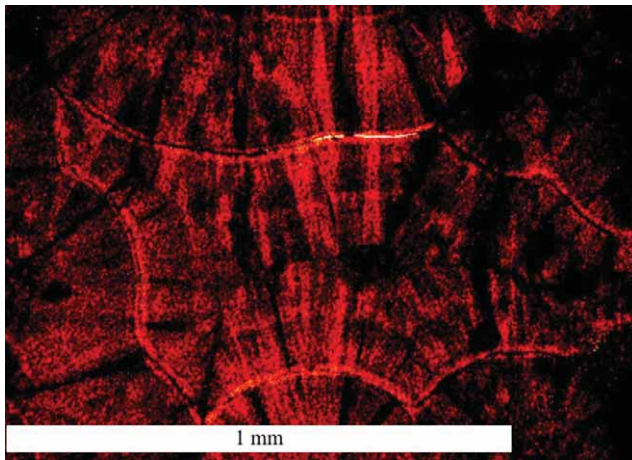**Figure 6:** Black and shiny kidney shaped concretions and glassy needles in compact limonite (sample TLIM).

Figure 7: Photomicrograph of the internal radiating structure of goethite concretions (N) in compact limonite (sample TLIM).
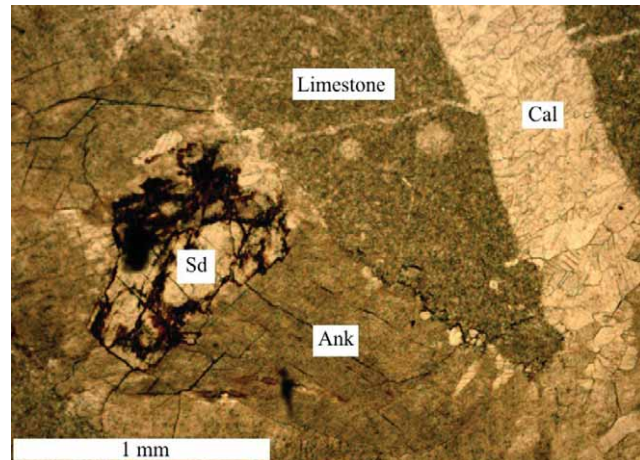

Figure 10: Photomicrographs of siderite (Sd), ankerite (Ank) and calcite (Cal) veins that cut limestone (sample TVAP1). Partial breakdown of siderite along cracks results in haematite occurrence (N+).

ance with the former more specific petrographic investigations of compact limonites performed by JURKOVIĆ (1961).

Pulverized limonite or "brand" (TBRA) from the Stojančići locality (Fig. 8) have also been studied in detail by JURKOVIĆ (1961) and therefore no new microscopic investigations of this sample have been made.

Common characteristics of the limestone sample (TVAP1) are veins bearing brown siderite, pale yellow ankerite, and tiny white calcite veinlets (Fig. 9). Macroscopic and microscopic structural relationships suggest that the siderite was partly replaced by ankerite, whereas calcite represents the youngest occurrence (Fig. 10). The limestone is dark gray micrite containing rare quartz grains, (up to 0.12 mm) and muscovite, (up to 0.06 mm). Only vein and veinlet free parts of the limestone were taken for chemical analysis.

The studied sample of carbonate shale (TVAP2) is composed of clay-sized grains, and is a dark, fissile, and laminated rock (Fig. 11). Microscopic study revealed that it consists of clay minerals, detrital quartz, muscovite and variously sized spherical and oval-shaped calcispheres, which are characteristically 60 to 300 μm in diameter (Fig. 12).

The sample of white-gray coloured ankerite (TMIX) shown in Figure 13 consists of an intimately associated white area of coarse grained ankerite crystals, with regular grain boundaries and a gray area of fine to medium grained ankerite with black lobate grain boundaries, and interstitial places filled with a clayey-carbonaceous substance and quartz ag-

Figure 8: Pulverized limonite or "brand" (sample TBRA).

Figure 9: Brown siderite and pale yellow ankerite veins and tiny white calcite veinlets that cut the studied limestone (sample TVAP1) .

Figure 11: Dark fissile laminate carbonate shale (sample TVAP1).

Garašić and Jurković: Geochemical characteristics of different iron ore types from the Southern Tomašica deposit, Ljubija, NW Bosnia

261

Geologia Croatica

gregates (Fig. 14). Relics of fine grained ankerite with lobate black grain boundaries have been observed within the white coarse grained ankerite. Ankerites of both, white and gray areas are characterized by undulose extinction. Due to the intimate association of the white and gray areas of this sample, one chemical analysis of a mixed area was made.

White coarse grained ankerite (sample TANK), occurs in the form of an irregular nest (Fig. 15) in the matrix of dark fine grained ankerite (sample TANK 1). White coarse grained ankerite is characterized by regular grain boundaries and grains free of inclusions. In contrast, grain boundaries of dark fine grained ankerite are highly irregular, and the interstitial space is filled with a clayey-carbonaceous substance containing usually small quartz grains and rarely muscovite (Fig. 16). Dark fine ankerite grains show locally tiny quartz inclusions. The undulose extinction is typical for both coarse and fine grained ankerite. Different parts of this non-homogeneous rock sample were carefully separated from each other for chemical analysis.

White coarse grained ankerite (sample TANMIC) also occurs in the form of an irregular nest, but this time in a matrix of reddish coarse grained siderite (sample TCOR), which

is surrounded by dark fine grained siderite (sample TMIC) as shown in Fig. 17. Various parts of this non-homogeneous rock sample were carefully separated for chemical analysis.
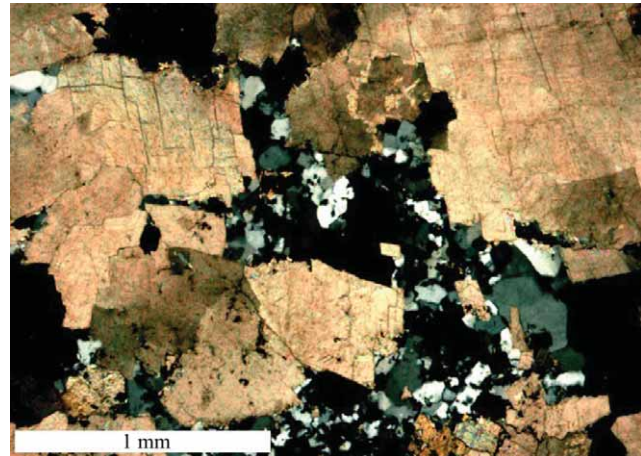
Figure 14: Photomicrograph of the fine to medium part of an ankerite sample TMIX with quartz aggregates filling interstitial places between ankerite grains having lobate grain boundaries (N+).
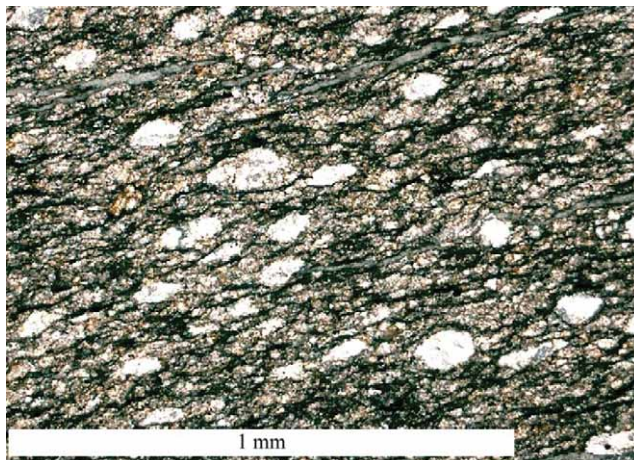
Figure 12: Photomicrograph of carbonate shale consisting of clay minerals, detrital quartz, muscovite and variously sized spherical and oval-shaped calcispheres (N+).

Figure 15: White coarse grained ankerite (sample TANK) occurs in form of an irregular nest in the matrix of dark fine grained ankerite (sample TANK1).

Figure 13: Intimately associated white coarse grained area and gray fine to medium grained area of ankerite (sample TMIX).

Figure 16: Photomicrograph of the boundary area between coarse grained ankerite (sample TANK) and fine grained ankerite (sample TANK 1). Grain boundaries of fine grained ankerite are highly irregular, the interstitial space is filled with a clayey-carbonaceous substance (N+).

White coarse grained ankerite and reddish coarse grained siderite are characterized by regular grain boundaries, whereas those of dark fine grained siderite are irregular with

Figure 17: White coarse grained ankerite (sample TANMIC) occurs in the form of an irregular nest in a matrix of reddish coarse grained siderite (sample TCOR) which is surrounded by dark fine grained siderite (sample TMIC).
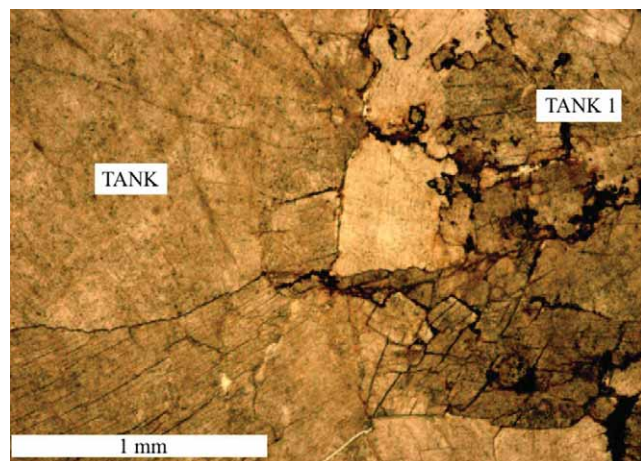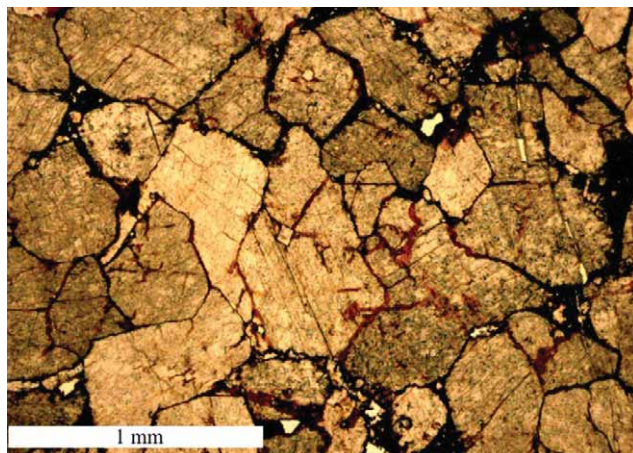

Figure 18: Photomicrograph of fine grained siderite (sample TMIC) with irregular grain boundaries and interstitial spaces filled with a clayey-carbonaceous substance and disseminated quartz grains. Red haematite occurs along cracks and cleavage of siderite because of weathering processes (N).

Figure 19: Yellow coarse grained siderite (sample AD-2) irregularly embedded in a matrix of reddish fine grained siderite from the Adamuša opencast mine.

interstitial spaces filled with a clayey-carbonaceous substance and disseminated quartz grains. Partial breakdown of both types of siderite results in the occurrence of haematite along grain boundaries, cleavage and cracks in the siderite (Fig. 18). Ankerite and both type of siderite are characterized by undulose extinction.

The sample of yellow coarse grained siderite (sample AD-2) irregularly embedded in a matrix of reddish fine grained siderite was collected in the Adamuša opencast mine (Fig. 19). Again, fine grained mineral is characterized by irregular boundaries and interstitial spaces filled with a clayey-carbonaceous substance and disseminated quartz grains, whereas the coarse grained mineral consists of polygonal grains. Chemical analysis of yellow coarse grained siderite was undertaken, although due to the intimate association of yellow and reddish siderite it is possible that a minor quantity of reddish siderite was included in the analysis.

Careful examination of mineral thin-sections using transmitted polarized light enabled separation of the fresh and weathered samples, and the different parts of non-homogeneous samples to be distinguished. Selected samples were crushed, hand–picked under binocular microscope and powdered in an agate mortar for chemical analysis.

Major, minor and trace element contents were determined by inductively coupled plasma mass spectrometry (ICP-MS) in the Acme Analytical Laboratories (Vancouver) Ltd in Canada. In the same laboratory the total organic carbon (TOT/C) and total sulphure (TOT/S) of all six samples were measured too.

4. ANALYTICAL RESULTS

4.1. Main oxides

The concentrations of many main oxides (SiO_2, Al_2O_3, TiO_2, Na_2O, K_2O) in compact limonite are slightly higher but very similar to those in siderite, limestone and dark fine grained ankerite (Table 1). Slightly lower concentrations of these oxides, (but still similar to those in siderite and limestone) are displayed in the white coarse grained ankerite. Pulverized limonite on the other hand differs significantly, relative to compact limonite. The SiO_2 component in pulverized limonite is enriched by 3 times, Al_2O_3 component by 10 times, Na_2O component by 7 times, K_2O component by 4 times and the P_2O_5 component by 20 times compared to compact limonite (Table 1). These elevated values are mostly comparable to carbonate shale which is even more enriched in the SiO_2 component (27.10 wt % compared to 16.73 wt % of pulverized limonite), but depleted in Al_2O_3 (only 4.99 wt % in comparison with 11.78 wt% of pulverized limonite). There are positive correlations between the Al_2O_3, K_2O and TiO_2 contents and the aluminosilicate fraction of the samples. The Fe_2O_3 and MgO contents in siderite vary from 3.09 and 5.11 wt%, to 51.66 and 58.34 wt% respectively. In ankerite, the Fe_2O_3 content ranges from 13.94 to 21.35 wt%. Its MgO content is between 9.29 and 10.41 wt%. MnO values are positively correlated with Fe_2O_3 in all samples. The highest MnO content is present in siderite (2.15 to 2.55 wt%). Ankerite

Garašić and Jurković: Geochemical characteristics of different iron ore types from the Southern Tomašica deposit, Ljubija, NW Bosnia

263

Geologia Croatica

shows lower MnO values (0.88 to1.10 wt%) and limestone has the lowest MnO value (0.10 wt%). The highest CaO content in siderite is found in the red coarse grained TCOR sample (3.98 wt%) in the immediate vicinity of the ankerite nests. The CaO content of the other two siderite samples varies from 1.34 to 1.63 wt%. Ankerite is characterized by a CaO content varying between 26.87 and 28.59 wt%. The greatest chemical differences between pulverized limonite and carbonate shale is visible in the content of Fe_2O_3 (3.27 wt% in carbonate shale and 53.87 wt% in pulverized limonite) and CaO (31.60 wt% in carbonate shale and 0.23 wt% in pulverized limonite).

4.2. REE content

The REE content of ankerite, limestone, siderite and compact limonite is low (up to 22.49 ppm), in contrast to pulverized limonite (118.45 ppm) and carbonate shale (72.99 ppm), as reported in Table 2. There is a clear positive correlation between the weight percent of the main oxides SiO_2 and Al_2O_3 and REE (Table 1, Table 2) in compact limonite, pulverized limonite and carbonate shale. This suggests REE concentration dependence of the clay component in the samples. However, the same correlation is not so obvious for carbonates.

The REE concentrations of all the studied samples are normalized to C1 chondrite (SUN & McDONOUGH, 1989), in order to compare fractionations of light REE $(La/Sm)_N$, heavy REE $(Gd/Yb)_N$, total REE $(La/Yb)_N$, Eu anomaly (Eu/

$Eu^* = Eu_N/\sqrt{(SmxGd)_N}$ and Ce anomaly $(Ce/Ce^* = Ce_N/(\sqrt{La} x Pr)_N)$ in different samples (Table 2).

The REE pattern of compact limonite is characterized by relatively low light $((La/Sm)_N = 2.87)$, heavy $((Gd/Yb)_N = 0.98)$ and total $((La/Yb)_N = 3.19)$ REE fractionations, a strong positive Eu anomaly $(Eu/Eu^* = 2.11)$ and weakly expressed negative Ce anomaly $(Ce/Ce^* = 0.82)$ as shown in Table 2 and Fig. 20a. The total concentration of REE is 18.78 ppm.

Limestone exhibits slightly lower REE abundance (Fig. 20b) and light REE fractionation $(La/Sm)_N = 2.29)$, but more strongly expressed heavy $((Gd/Yb)_N = 2.31)$ and total $((La/Yb)_N = 5.08)$ REE fractionation compared to compact limonite. Its Eu anomaly $(Eu/Eu^* = 1.12)$ is positive, but very weak, whereas the Ce anomaly $(Ce/Ce^* = 0.68)$ is negative and stronger than in compact limonite. The overall REE content is 9.15 ppm.

Studied coarse and fine siderite samples do not show differences in their REE patterns (Fig. 20c). They all display significant enrichment of LREE over HREE $((La/Yb)_N = 3.36–3.91, (La/Sm)_N = 1.29–1.97, (Gd/Yb)_N = 1.18–2.21)$, a pronounced positive Eu anomaly $(Eu/Eu^* = 2.24–3.40)$ and a small negative Ce anomaly $(Ce/Ce^* = 0.78–0.87)$. Their total REE concentrations vary from 13.71 to 13.23 ppm.

In contrast to the REE patterns seen in siderite, those in ankerite show a clear distinction between fine grained and coarse grained samples (Fig. 20d). The REE pattern of fine

Table 1: The main element content of the studied samples.

Sample	MDL	TLIM	TBRA	TVAP1	TVAP2	TMIX	TANK	TANMIC	TANK 1	TCOR	TMIC	AD-2
mineral/ rock		compact limonite	pulverized limonite	limestone	carbonate shale	ankerite	ankerite	ankerite	ankerite	siderite	siderite	siderite
						white gray fine to coarse grained	white coarse grained	white coarse grained	dark fine grained	red coarse grained	dark fine grained	yellow coarse grained
	wt.%	wt.%	wt.%	wt.%	wt.%	wt.%	wt.%	wt.%	wt.%	wt.%	wt.%	wt.%
SiO_2	0.01	4.98	16.73	3.51	27.1	2.23	0.31	0.10	4.96	3.64	3.36	1.77
Al_2O_3	0.01	1.12	11.78	0.28	4.99	0.24	0.05	0.05	0.57	0.49	0.48	0.27
Fe_2O_3	0.04	79.61	53.87	0.87	3.27	18.41	16.91	21.35	13.94	51.66	54.41	58.34
MgO	0.01	0.13	0.74	0.61	2.08	9.47	10.41	9.29	10.29	4.99	5.11	3.09
CaO	0.01	0.15	0.23	52.24	31.6	27.18	28.59	26.87	28.47	3.98	1.63	1.34
Na_2O	0.01	0.03	0.15	0.03	0.12	0.05	0.05	0.04	0.04	0.04	0.03	0.04
K_2O	0.01	0.29	1.38	0.08	1.36	0.06	0.01	0.01	0.16	0.13	0.14	0.07
TiO_2	0.01	0.05	0.47	<0.01	0.19	<0.01	<0.01	<0.01	0.02	0.01	0.02	0.01
P_2O_5	0.01	<0.01	0.22	0.02	0.06	<0.01	<0.01	<0.01	<0.01	0.03	0.02	<0.01
MnO	0.01	0.84	0.82	0.10	0.28	1.01	0.97	1.10	0.88	2.19	2.15	2.55
Cr_2O_3	0.002	<0.002	0.01	<0.002	0.007	<0.002	<0.002	<0.002	<0.002	<0.002	<0.002	<0.002
LOI	−5.1	12.70	13.40	42.10	28.80	41.20	42.50	41.10	40.50	32.70	32.60	32.4
Σ	0.01	99.90	99.80	99.84	99.86	99.85	99.80	99.91	99.83	99.86	99.95	99.88
TOT/C	0.02	0.27	0.44	11.74	8.28	11.77	12.22	11.96	11.43	10.40	10.59	10.43
TOT/S	0.02	<0.02	<0.02	<0.02	0.70	<0.02	<0.02	<0.02	0.03	<0.02	<0.02	0.03

Table 2: Rare earth element composition of the studied samples.

Sample	MDL	TLIM	TBRA	TVAP1	TVAP2	TMIX	TANK	TANMIC	TANK 1	TCOR	TMIC	AD-2
mineral/ rock		compact limonite	pulverized limonite	limestone	carbonate shale	ankerite	ankerite	ankerite	ankerite	siderite	siderite	siderite
						white gray fine to coarse grained	white coarse grained	white coarse grained	dark fine grained	red coarse grained	dark fine grained	yellow coarse grained
	ppm	ppm	ppm	ppm	ppm	ppm	ppm	ppm	ppm	ppm	ppm	ppm
La	0.10	3.60	27.3	1.70	16.30	1.40	<0.10	<0.10	1.20	2.20	2.60	1.80
Ce	0.10	5.50	42.6	2.40	27.70	3.90	0.40	0.10	2.30	4.10	5.10	3.80
Pr	0.02	0.75	6.16	0.44	3.55	0.86	0.14	0.06	0.44	0.75	0.86	0.63
Nd	0.30	3.20	22.3	1.80	13.80	4.60	1.00	0.80	2.40	3.10	4.40	2.90
Sm	0.05	0.81	4.79	0.48	2.57	1.91	0.62	1.57	0.87	0.72	0.95	0.90
Eu	0.02	0.61	1.57	0.21	0.87	1.72	0.50	1.91	0.65	0.51	0.74	0.99
Gd	0.05	0.96	3.97	0.67	2.54	2.58	0.81	2.87	1.19	0.67	0.85	0.88
Tb	0.01	0.18	0.63	0.10	0.40	0.45	0.15	0.55	0.18	0.12	0.15	0.13
Dy	0.05	1.06	3.64	0.58	2.14	2.31	0.77	3.09	1.01	0.75	0.97	0.67
Ho	0.02	0.25	0.73	0.13	0.43	0.47	0.15	0.59	0.19	0.17	0.22	0.14
Er	0.03	0.81	2.03	0.32	1.23	1.20	0.43	1.82	0.52	0.50	0.62	0.41
Tm	0.01	0.13	0.34	0.05	0.19	0.16	0.07	0.26	0.08	0.09	0.10	0.07
Yb	0.05	0.81	2.08	0.24	1.10	0.82	0.35	1.34	0.40	0.47	0.53	0.33
Lu	0.01	0.11	0.31	0.03	0.17	0.11	0.05	0.19	0.06	0.08	0.08	0.06
ΣPEE		18.78	118.45	9.15	72.99	22.49	5.54	15.25	11.49	14.23	18.17	13.71
Eu/Eu*		2.11	1.10	1.13	1.04	2.37	2.16	2.75	1.95	2.24	2.52	3.40
Ce/Ce*		0.82	0.80	0.68	0.89	0.87	0.83	0.32	0.78	0.78	0.84	0.87
$(La/Yb)_N$		3.19	9.41	5.08	10.63	1.22	0.20	0.05	2.15	3.36	3.52	3.91
$(La/Sm)_N$		2.87	3.68	2.29	4.09	0.47	0.10	0.04	0.89	1.97	1.77	1.29
$(Gd/Yb)_N$		0.98	1.58	2.31	1.91	2.60	1.91	1.77	2.46	1.18	1.33	2.21

grained ankerite (sample TANK1) is similar to the siderite patterns showing enrichment of LREE over HREE ($(La/Yb)_N$ = 2.15), the positive Eu anomaly (Eu/Eu* = 1.95) and the negative Ce anomaly (Ce/Ce* = 0.78). Differences exist in its lower $(La/Sm)_N$ ratio (0.89) and greater $(Gd/Yb)_N$ ratio (2.46) compared with siderite. Its ΣREE is 11.49 ppm. In contrast, two coarse grained ankerite samples (samples TANK and TANMIC) exhibit remarkable depletion of LREE over HREE ($(La/Yb)_N$ = 0.05–0.20), a strong reverse LREE pattern ($(La/Sm)_N$ = 0.04–0.10) and $(Gd/Yb)_N$ ratios ranging from 1.77 to 1.91. The coarse grained ankerite samples are like other studied samples characterized by positive Eu anomaly (Eu/Eu* = 2.16–2.75) and negative Ce anomaly (Ce/Ce* = 0.32–0.83) and their ΣREE vary between 5.54 and 15.25. The TMIX sample consisting of fine to coarse grained ankerite possesses the highest REE abundance (ΣREE = 22.49 ppm) among the studied ankerite samples and has characteristics similar to those of fine grained ankerite (slight enrichment of LREE over HREE ($(La/Yb)_N$ = 1.22), a positive Eu anomaly (Eu/Eu* = 2.37), negative Ce anomaly (Ce/Ce* = 0.87), low $(La/Sm)_N$ ratio (0.47) and greater $(Gd/Yb)_N$ ratio (2.60)).

In contrast to all other samples, pulverized limonite (Fig. 20a) and carbonate shale (Fig. 20b) show completely different REE patterns and abundances (up to 6 to 13 times higher relative to other samples) (Fig. 20c,d). Although pulverized limonite is characterized by the highest REE abundance (ΣREE = 118.45) its REE fractionation patterns ($(La/Sm)_N$ = 3.68, $(Gd/Yb)_N$ = 1.58, $(La/Yb)_N$ = 9.41), a slightly positive Eu anomaly (Eu/Eu* = 1.10) and small negative Ce anomaly (Ce/Ce* = 0.81) are similar to those in the carbonate shale ($(La/Sm)_N$ = 4.09, $(Gd/Yb)_N$ = 1.91, $(La/Yb)_N$ = 10.63, (Eu/Eu* = 1.04, (Ce/Ce* = 0.89).

4.3. Other trace elements

The content of Rb, Cs, Ba and Ga are characterized by a positive correlation with K_2O and Al_2O_3 values, pointing to the aluminosilicate fraction of the samples. Consequently, the pulverized limonite contains the highest values of Rb (74.2 ppm), Cs (14.8 ppm), Ba (227 ppm) and Ga (14.1 ppm). It is also characterized by the highest concentrations of V (104 ppm), Zr (115.2 ppm) and Y (19.3 ppm).
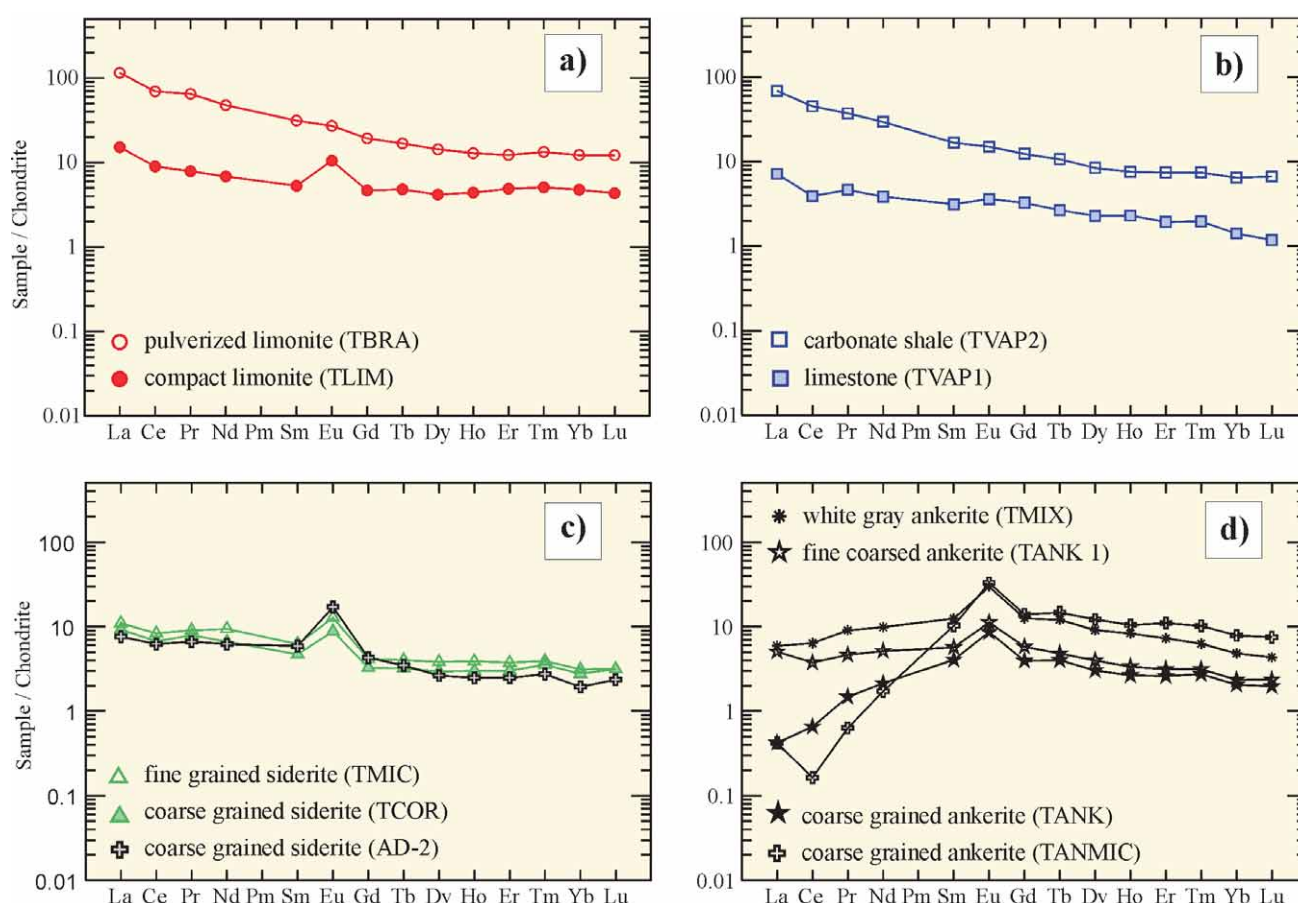
Garašić and Jurković: Geochemical characteristics of different iron ore types from the Southern Tomašica deposit, Ljubija, NW Bosnia

265

Geologia Croatica

Figure 20: Plot of rare-earth elements normalized to C1 chondrites (SUN & McDONOUGH, 1989) in: a) compact and pulverized limonite; b) limestone and carbonate shale; c) siderite; d) ankerite.

The Sr content increases with the increasing calcium content of the samples due to the crystal chemical control. Consequently the Sr content increases from siderite (12.3 to 14.9 ppm), and ankerite (42.4 to 79.5 ppm) to being highest in the limestone (1051 ppm).

The concentrations of Co, Ni, Pb, Zn and As, show a positive correlation with Fe_2O_3 in siderite samples, whereas in the ankerite samples such correlation doesn't exist. The content of Co, Ni and As in ankerite samples are positively correlated with Al_2O_3 and SiO_2 components, whereas the Pb, Zn and Cu contents are most likely linked to the presence of tiny sulphides near the grain boundaries. The highest values of Ni (36.4 ppm), Pb (116.6 ppm), Zn (345 ppm), As (382.8 ppm) and Cu (52.4 ppm) are found in pulverized limonite, whereas the carbonate shale is characterized by the highest content of Co (25.9 ppm).

The compact limonite contains elevated concentrations of many trace elements (Cs, Ga, Hf, Rb, Th, V, Zr,Y, Cu, Zn, Ni and Sb) relative to siderite, ankerite and limestone (Table 3). In the same comparison the highest contents of Co (5.60 ppm) and As (4.60 ppm) are found in siderite, of Hg (0.14 ppm) in ankerite and of U (1.60 ppm) and Pb (11.1 ppm) in the limestone.

In comparison with compact limonite, siderite, ankerite and limestone the concentrations of Ni, Co, Cs, Ga, Hf, Nb, Rb, Ta, Th, U, V, W. Zr, Y, Mo, Cu, Pb, Zn, As, Sb and Hg are even more elevated in the pulverized limonite and carbonate shale (Table 3). The only elements having higher concentrations in the carbonate shale than in pulverized limonite are Co, Bi, Ag, Hg and Se (Table 3).

5. DISCUSSION

Geochemical investigations of two limonite ore types show considerable differences in the content of their main elements, REE and other trace elements. In order to constrain their possible lithotype sources, the geochemical characteristics of studied siderite, ankerite, host limestone and carbonate shale are further discussed.

5.1. REE chemistry of carbonate phases

Generally, many factors may influence the REE content of carbonate minerals. The most important include the size of sites occupied by REE ions in the crystal lattice, REE chemistry of mineralizing fluids and REE partitioning between the precipitating mineral and mineralizing fluid (MÖLLER, 1983). In addition, according to MÖLLER et al. (2004), REE abundances are higher in hydrothermal than in cold fluids and increase with decreasing pH (MICHARD, 1989). In acid solutions LREEs are enriched relative to HREEs,

whereas alkaline solutions exhibit depletion of the LREEs over HREEs usually having La/Lu < 1 (SCHWINN & MARKL, 2005).

In the context of crystal chemistry, calcite should be characterized by enrichment of LREE over HREE in contrast to siderite that should display depletion of LREE over HREE.

Table 3: Trace element content of the studied samples.

Sample	MDL	TLIM	TBRA	TVAP1	TVAP2	TMIX	TANK	TANMIC	TANK 1	TCOR	TMIC	AD-2
mineral/ rock		compact limonite	pulverized limonite	limestone	carbonate shale	ankerite	anker-ite	ankerite	ankerite	siderite	siderite	siderite
						white gray fine to coarse grained	white coarse grained	white coarse grained	dark fine grained	red coarse grained	dark fine grained	yellow coarse grained
	ppm	ppm	ppm	ppm	ppm	ppm	ppm	ppm	ppm	ppm	ppm	ppm
Sc	1.0	2.0	12.0	<1.0	5.0	<1.0	<1.0	<1.0	<1.0	<1.0	<1.0	1.0
Ba	1.0	201.0	227.0	26.0	140.0	24.0	5.0	8.0	18.0	17.0	21.0	44.0
Be	1.0	1.0	2.0	<1.0	<1.0	<1.0	<1.0	<1.0	<1.0	<1.0	<1.0	<1.0
Co	0.2	2.7	18.1	0.2	25.9	2.7	0.5	0.8	4.1	3.6	5.6	11.7
Cs	0.1	1.8	14.8	0.4	9.3	0.4	0.2	0.2	0.6	0.7	0.7	0.3
Ga	0.5	3.2	14.1	0.5	7.4	0.6	0.5	0.5	1.0	2.7	3.1	3.9
Hf	0.1	0.5	3.3	0.1	1.0	0.1	0.1	0.1	0.2	0.2	0.2	0.1
Nb	0.1	1.0	10.2	0.3	4.1	0.2	0.1	0.1	0.5	0.3	0.3	0.4
Rb	0.1	11.9	74.2	3.2	55.0	2.4	0.5	0.5	6.3	5.1	5.5	3.2
Sn	1.0	<1.0	3.0	1.0	1.0	1.0	1.0	1.0	1.0	1.0	1.0	<1.0
Sr	0.5	7.3	42.4	1051.1	357.3	55.1	79.5	42.4	66.5	14.4	12.3	14.9
Ta	0.1	<0.1	0.8	0.1	0.3	0.1	0.1	0.1	0.1	0.1	0.1	<1.0
Th	0.2	1.0	8.9	0.3	4.0	0.5	0.2	0.2	0.3	0.6	0.6	0.5
U	0.1	0.9	5.5	1.6	4.6	0.7	0.1	0.1	0.1	0.4	0.5	2.5
V	8.0	19.0	104.0	8.0	70.0	8.0	8.0	8.0	8.0	8.0	11.0	12.0
W	0.5	<0.5	1,5	0.5	1.2	0.5	0.5	0.5	0.5	0.5	0.5	<0.5
Zr	0.1	20.0	115.2	2.3	31.9	1.6	1.0	0.4	5.9	5.3	6.6	4.4
Y	0.1	7.7	19.3	4.8	14.0	15.3	5.5	17.8	7.8	5.0	5.8	4.8
Mo	0.1	<0.1	2.5	0.1	9.9	0.1	0.2	0.1	0.8	0.2	0.3	0.5
Cu	0.1	9.3	52.4	0.7	22.7	2.6	2.2	30.7	3.5	2.4	1.5	1.6
Pb	0.1	3.4	116.6	11.1	54.3	1.7	1.8	1.8	5.0	1.3	1.5	136.7
Zn	1.0	57.0	345.0	14.0	25.0	14.0	22.0	14.0	17.0	24.0	35.0	46.0
Ni	0.1	10.7	36.4	1.2	35.6	4.3	1.1	1.6	6.3	5.4	7.2	11.6
As	0.5	1.2	382.8	0.5	34.8	4.3	0.5	0.5	6.7	3.6	4.6	5.5
Cd	0.1	<0.1	0.2	0.1	0.1	0.1	0.1	0.1	0.1	0.1	0.1	<1.0
Sb	0.1	0.8	3.5	0.3	4.5	0.2	0.1	0.1	1.2	0.1	0.2	0.6
Bi	0.1	<0.1	0.3	0.1	0.9	0.1	0.1	0.1	0.2	0.1	0.1	<1.0
Ag	0.1	<0.1	0.1	0.1	0.8	0.1	0.1	0.1	0.1	0.1	0.1	<1.0
Au* (ppb)	0.5	<0.5	0.5	0.5	0.5	0.5	0.5	0.5	0.5	1.5	0.5	<0.5
Hg	0.01	0.04	0.52	0.05	0.7	0.05	0.13	0.01	0.14	0.03	0.03	0.09
Tl	0.1	<0.1	0.3	0.1	0.2	0.1	0.1	0.1	0.1	0.1	0.1	<1.0
Se	0.5	<0.5	0.5	0.5	1.9	0.5	0.6	0.5	0.5	0.5	0.5	<0.5
Zr/TiO$_2$		0.040	0.025	>0.023	0.017	>0.016	>0.010	>0.004	0.030	0.053	0.033	0.044
Zr/Nb		20.000	11.290	7.670	7.780	8.000	10.000	4.000	11.800	17.670	22.00	11.000
Nb/Y		0.130	0.530	0.060	0.290	0.010	0.020	0.010	0.060	0.060	0.050	0.080

Ankerite should show intermediate characteristics between these two patterns. The larger Ca ion site in calcite incorporates larger LREEs more easily, whereas the smaller Fe ion site in siderite easily incorporates smaller HREEs.

Thus the LREE enrichment in siderite (Fig. 20), and its overall greater REE content (ΣREE = 13.71–18.17 ppm) in comparison with limestone (ΣREE = 9.15 ppm), could not be solely attributed to crystallographic control, but indicates the precipitation of siderite from an LREE enriched parent fluid. Strong depletion of LREE over HREE $((La/Yb)_N = 0.05–0.20)$ in the two white coarse grained ankerites on the other hand reveals that they were precipitated either from a colder and more alkaline mineralizing fluid, or from a fluid with a different source relative to siderite and fine grained ankerite.

The negative Ce anomaly, being the result of the oxidation of Ce^{3+} to Ce^{4+} and its consequent removal from the solution as CeO_2, is typical for marine limestones (HU et al., 1988). The studied limestone exhibits a pronounced negative Ce anomaly (0.68) and weak positive Eu anomaly (1.13). The negative Ce anomaly, although weaker, is present in siderite (0.78–0.87), fine grained ankerite (0.78), and also in one coarse grained ankerite (0.83). Its lower values relative to limestone could be explained by lower pH or a lower pO_2 of mineralizing fluids from which siderite and ankerite samples precipitated. The presence of a significant negative Ce anomaly (0.32) in the TANMIC sample (coarse grained ankerite) indicates more oxygenated conditions for its precipitation.

The additional noticeable feature in the studied carbonate REE patterns is a pronounced positive Eu anomaly in siderite (2.24–3.40) and coarse grained ankerite (2.16–2.75). It is weaker in the fine grained ankerite (1.95) and weakest in the limestone (1.13). Numerous analyses of REE concentrations in hydrothermal fluids along oceanic ridges (MICHARD & ALBAREDE, 1986; CAMPBELL et al., 1988) revealed that hydrothermal fluids are enriched in ΣREE (10–10^4 times relative to seawater concentrations), and are characterized by a significant positive Eu anomaly (OLIVAREZ & OWEN, 1991). Furthermore, textural evidence (the occurrence of veins and nests) in the studied siderite and ankerite samples from the Olistostrome member in Javorik Formation support the hydrothermal origin. The interaction between some Eu-rich mineralizing fluid and limestone could be reflected in the LREE depletion of ankerite, due to effective HREE complexion. Additionally, the strong similarity in the content and the fractionation of HREE in fine grained ankerite and limestone (Fig. 20) might also indicate the possible involvement of limestone in the origin of ankerite. The analytical results obtained are in accordance with those published by STRMIĆ PALINKAŠ et al. (2009) who suggested a hydrothermal-metasomatic origin of the Fe mineralization. However, it should be emphasized that there was more than one hydrothermal stage. This is reflected in ore texture (fine grained, coarse grained, veins, nests), colour (white, gray, red) and chemical features. Significantly lower Al_2O_3 values occur in white coarse grained ankerite (0.05 wt.%) when compared to those in fine grained ankerite (0.57

wt%) and siderite (0.27–0.49 wt%). However, due to the lack of a clear positive correlation between wt% Al_2O_3 and ΣREE (see Table 1 and 2) it seems that the REEs are not hosted in detrital phases of carbonate samples.

5.2. REE chemistry of compact limonite

The REE pattern of compact limonite $((La/Sm)_N = 2.87$, $(Gd/Yb)_N = 0.98$, $(La/Yb)_N = 3.19$, Eu/Eu* = 2.11, Ce/Ce* = 0.82) and its other trace element content (Table 3), exhibits the closest genetic relationship with siderite. Chemical weathering of siderite most probably resulted in its extensive supergene modification and the origin of compact limonite. Textural relationships and field occurrences of siderites and compact limonite support such a concept. It is also in accordance with the opinions of earlier investigators in this area (JURKOVIĆ, 1961; GRUBIĆ & PROTIĆ, 2003). The formation of limonite due to siderite weathering is observed and documented in many other geological environments (MORRIS, 1980).

5.3. REE chemistry of carbonate shale and pulverized limonite

Considering the fractionation of light REE $(La/Sm)_N$, heavy REE $(Gd/Yb)_N$ and total REE $(La/Yb)_N$ when normalized to chondrite (SUN & McDONOUGH, 1989), the REE pattern of the studied carbonate shale is similar to those of the North American Shale Composite (NASC – GROMET, 1984), and the Post Archean Australian Shale (PAAS – McLENNAN, 1989) as shown in Fig. 21. The most remarkable difference is the absence of the pronounced negative Eu anomaly in the carbonate shale, which is typical for NASC and PAAS. Carbonate shale displays almost no Eu anomaly (Eu/Eu* = 1.04) and has a small negative Ce anomaly (Ce/Ce* = 0.89).

An analogous REE pattern, but with enhanced overall REE content, is shown by pulverized limonite (Eu/Eu* = 1.10; (Ce/Ce* = 0.81). Consequently, the carbonate shale might be one of the suitable lithotypes for providing the REE content to pulverized limonite. GRUBIĆ & PROTIĆ (2003)
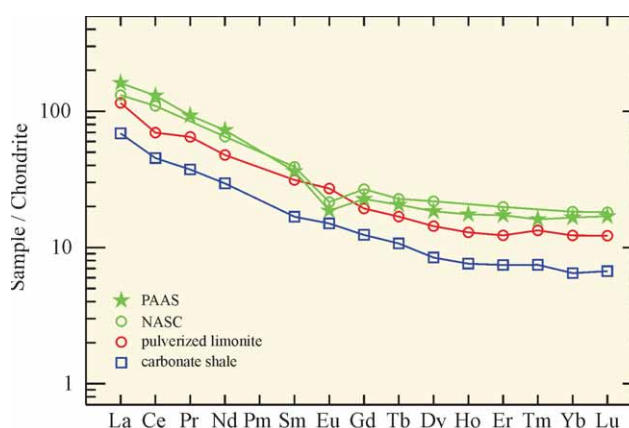

Figure 21: Plot of rare-earth elements normalized to C1 chondrites (SUN & McDONOUGH, 1989) in compact and pulverized limonite compared with the REE pattern of North American Shale Composite (NASC – GROMET, 1984) and Post Archean Australian Shale (PAAS – McLENNAN, 1989).

described comb-textured ankerite and dolomite limestone being completely enclosed by pulverized limonite. Therefore they concluded that the weathering of ankerite led to the formation of pulverized limonite. The REE pattern of pulverized limonite analysed in this study differs strongly from the REE patterns of any ankerite types analysed here and hence would contradict such a conclusion. However, it has to be emphasized that the analysed sample of pulverized limonite (TBRA) was not taken in its original place of formation, but in the Pleistocene–Quaternary lake limonite deposit (Stojančići location). During transportation by rain, river or wind, pulverized limonite could become more or less contaminated. The enhanced overall REE content in pulverized limonite (ΣREE = 118.45 ppm) relative to compact limonite (18.78 ppm), may be explained by such crustal rock contamination.

5.4. Other trace elements

Considerably higher concentrations of other trace elements in siderite samples (Co = 3.6–11.7 ppm; Ni = 5.4–11.6 ppm; Rb = 3.2–5.5 ppm; Zr = 4.4–6.6 ppm), and fine grained ankerite (Co = 4.1 ppm; Ni = 6.3 ppm; Rb = 6.3 ppm; Zr = 5.9 ppm), relative to those in white coarse ankerite (Co = 0.5–0.8 ppm; Ni = 1.1–1.6 ppm; Rb = 0.5 ppm; Zr = 0.4–1.0 ppm), support the hypothesis of the precipitation of fine grained ankerite and white coarsed ankerite from different mineralizing fluids.

Trace elements are in general depleted in compact limonite relative to pulverized limonite. The high values of Zr (115.2 ppm) in pulverized limonite indicate the possible presence of a clastic component of igneous origin, whereas high values of Rb (74.2 ppm), Sr (42.4 ppm), Th (8.9 ppm) indicate components derived by weathering from crustal felsic rocks. The enhanced concentrations of Cu (52.4 pppm), Pb (112 ppm), Zn (345 ppm) and As (382.8 ppm) may be attributed to the presence of components arising from the weathering of sulphide minerals.

The ratios of some immobile trace elements such as Zr/TiO_2 and Nb/Y are regarded as very useful for protolith determination (WINCHESTER & FLOYD, 1977) because they don't change during weathering processes. The values of the Zr/TiO_2 ratio in compact limonite (0.040) and siderite (between 0.033 and 0.053), are in concordance with the postulated origin of compact limonite from siderite. In the fine grained ankerite (sample TANK1), the Zr/TiO_2 ratio is 0.030, whereas in the coarse grained ankerite it varies between 0.004 and 0.010. As pulverized limonite has a Zr/TiO_2 ratio of 0.025, only fine grained ankerite or carbonate shale (0.017) might be regarded as its possible protolith. Similar conclusions could be drawn on the basis of the Zr/Nb ratio which in siderite varies from 11 to 22 and in compact limonite is 20. In the pulverized limonite, the Zr/Nb ratio is 11.29, in carbonate shale 7.78, in the fine grained ankerite 11.8, and in the coarse grained ankerite it ranges between 4 and 10. However, the values of the Nb/Y ratios in pulverized limonite (0.53), carbonate shale (0.29), compact limonite (0.13), siderites (0.05–0.08), fine grained ankerite (0.06) and

coarse grained ankerite (0.01–0.02) do not support the possibility of the origin of pulverized limonite through the weathering processes of ankerites.

5.5. Field relationships and geochemical data

The field relationship between siderite and compact limonite, is consistent with the conclusion based on REE geochemistry, that compact limonite most probably originated by the alteration of siderite. Compact limonite occurs as gossan formed in situ on siderite.

Pulverized limonite occurs in the field as bedded and lensoid shape deposits in palaeolakes, but also enclosing ankerite relics and ankeritic limestone in the Olistostrome member. The analyzed sample of pulverized limonite from a limonite deposit from the palaeolake exhibits significantly distinct REE patterns relative to any ankerite types studied in this paper.

Carbonate shale is part of a flysch groundmass of the Olistostrome member in which carbonate olistolith fragments, blocks and their mineralized parts are embedded. The remarkable resemblance of its REE pattern with that of pulverized limonite indicates the possibility that pulverized limonite may generally originate by the alteration of a carbonate shale or flysch groundmass.

6. CONCLUSION

Two studied types of limonite ore from the Southern Tomašica mine display a notably distinct REE pattern, REE fractionations, Eu anomalies and contents of other trace elements and main oxides. The compact limonite formed in situ on siderite is characterized by remarkable lower overall REE abundances, lower LREE fractionation, lower and opposite HREE fractionation, a more strongly expressed positive Eu anomaly and far lower overall content of other trace elements compared to pulverized limonite. This supports the hypothesis of different protolith material for the two different limonite ore types.

The REE pattern of compact limonite and siderite almost overlap, supporting the interpretation of former investigators (JURKOVIĆ, 1961; GRUBIĆ & PROTIĆ, 2003) who concluded that compact limonite originated by the alteration of siderite.

The REE pattern of pulverized limonite on the other hand clearly differs from that of ankerite, which GRUBIĆ & PROTIĆ (2003) regarded as the protolith of pulverized limonite. On the basis of the similarity of their REE patterns, other trace element contents and Zr/TiO_2 ratios, carbonate shale might be regarded as a potential protolith of pulverized limonite. Alternatively, assuming that the analysed samples of pulverized limonite, collected in the Pleistocene–Quaternary lake limonite deposit, were contaminated during transportation by rain, river or wind, fine grained ankerite might also, on the basis of its Zr/TiO_2 ratio and Eu and Ce anomaly, be a potential protolith of pulverized limonite.

In order to develop full understanding of the formation of all limonite types in this area, the REE pattern and con-

269

Garašić and Jurković: Geochemical characteristics of different iron ore types from the Southern Tomašica deposit, Ljubija, NW Bosnia

Geologia Croatica

tent of other trace elements in siderite occuring as lenses in the lowest parts of the geological column of Southern Tomašica, and in the superposed limonite (Siderite-limonite member) and in pulverized limonite enclosing ankerite relicts (Olistostrome member) remain to be investigated.

ACKNOWLEDGEMENT

REFERENCES

BOROJEVIĆ ŠOŠTARIĆ, S. (2004): Geneza sideritno-baritno-polisulfidnih rudnih ležišta u paleozoiku Unutrašnjih Dinarida [*Genesis of siderite-barite-polysulfide ore deposit in Paleozoic of Inner Dinarides* – in Croatian].– Unpubl. Master Theses, University of Zagreb, Zagreb, 120 p.

CAMPBELL, A.C., PALMER, M.R., KLINKHAMMER, G.P., BOWERS, T.S., EDMOND, J.M., LAWRENCE, J.R., CASEY, J.F., THOMPSON, G., HUMPHRIS, S., RONA, R & KARSON, J.A. (1988): Chemistry of hot springs on the Mid-Atlantic Ridge.– Nature, 335, 514–519.

CVIJIĆ, R. (1986): Mineralni pigmenti ljubijske metalogenetske oblasti [*Mineral pigments of Ljubija metallogenic province* – in Serbian].– XI kongres geologa Jugoslavije, Tara 1986, Knjiga 4, 114–127.

CVIJIĆ, R. (2001): Mineralni resursi željeza, pelitoidne rude Ljubijske metalogenetske oblasti i perspektive razvoja [*Iron ore resurses, pelitoid ores of the Ljubija metallogenic province and perspective of the development* – in Serbian with English summary].– PhD Thesis, Faculty of Mining and Geology, Belgrade, 154 p.

GRADSTEIN, F., OGG, J. & SMITH, A. (2006): A Geologic Time Scale.– Cambridge, University Press, 589 p.

GROMET, L.P., DYMEK, R.F., HASKIN, L.A. & KOROTEV, R.L. (1984): The "North American Shale Composite": its compilation, major and trace element characteristics.– Geochim. Cosmochim. Ac., 48, 2469–2482.

GRUBIĆ, A. & PROTIĆ, LJ. (2003): Studija strukturnih i genetskih karakteristika Tomašičkog rudnog polja [*The study of structural and genetical characteristics of Tomašica ore field* – in Serbian].– In: GRUBIĆ, A. & CVIJIĆ, R. (eds.): Novi prilozi za geologiju i metalogeniju rudnika gvožđa "Ljubija" [*New Contribution to the Geology and Metallogeny of the Ljubija Iron Ore Mine* – in Serbian]. Institute of Mining Prijedor and Mines of Iron ore "Ljubija" Prijedor, Prijedor, 63–134.

GRUBIĆ, A., PROTIĆ, LJ., FILIPOVIĆ, I. & JOVANOVIĆ, D. (2000): New data on the Paleozoic of the Sana-Una area.– In: Proceedings of the International symposium Geology and Metallogeny of the Dinarides and the Vardar zone, ANURS, Banja Luka, 49–54.

HU, X., WANG, Y.L. & SCHMITT, R.A. (1988): Geochemistry of sediments on the Rio Grande Rise and the redox evolution of the South Atlantic Ocean.– Geochim. Cosmochim. Ac., 52, 201–207.

JURIĆ, M. (1967): Izvještaj o regionalnim istraživanjima paleozoika Sane u 1966. godini [*Report about the regional studies of Sana Palaeozoic in year 1966* – in Serbian].– Geološki zavod u Sarajevu. Izvještaj u fondu stručnih dokumenata RŽR Ljubija, Prijedor.

JURIĆ, M. (1969): Rudna ležišta o naslagama Omarsko–Prijedorskog polja [*Ore deposits about the sequences of Omarska-Prijedor field*].– Geol. glasnik, 13, 271–291, Sarajevo.

JURIĆ, M. (1971): Geologija područja sanskog paleozoika u sjeverozapadnoj Bosni [*Geology of Sana Palaeozoic area in NW Bosnia* – in Croatian].– Geološki glasnik XI, Sarajevo, 146 p.

JURKOVIĆ, I. (1961): Minerali željeznih rudnih ležišta Ljubije kod Prijedora [*Minerals of Ljubija iron ore deposit near Prijedor* – in Croatian with English summary].– Geol. vjesnik, 14, 161–220.

LOGOMERAC, V. (1960): Priprema Ljubijske sitnozrne rude "Branda" za preradu u visokoj peći [*Preparation of the fine-grained Ljubija ore "Brand" for the processing in blast furnace*].– Elaborat, Fond dokumenata "Željezara Sisak", 97 p.

McLENNAN, S.M. (1989): Rare earth elements in sedimentary rocks: influence of provenance and sedimentary processes.– In: LIPIN, B.R. & McKAY, G.A. (eds.): Geochemistry and mineralogy of rare earth elements. Reviews in Mineralogy, 21, 169–200.

MICHARD, A. & ALBAREDE, F. (1986): The REE content of some hydrothermal fluids.– Chem. Geol., 55, 51–60.

MICHARD, A. (1989): Rare earth element systematics in hydrotehrmal fluids.– Geochim. Cosmochim. Ac., 53, 745–750.

MÖLLER, P. (1983): Lanthanoids as a geochemical probe and problems in lanthanoid geochemistry-distribution and behavior of lanthanoids in non-magmatic phases.– In: SINHA, S.P. (ed.): Systematics and the properties of the Lanthanides, NATO Advanced Studies Institute Series, Series C, Mathematics and Physics Sciences, 109, 561–616.

MÖLLER, P., DULSKI, P., SAVASCIN, Y., CONRAD, M. (2004): Rare earth elements, yttrium and Pb isotope ratios in thermal spring and well waters of West Anatolia, Turkey: a hydrochemical study of their origin.– Chem. Geol., 206, 97–118.

MORRIS, R.C. (1980): A textural and mineralogy study of the relationship of iron ore to banded-iron formations in the Hamersley Iron Province of Western Australia.– Econ. Geol., 75, 184–209.

OLIVAREZ, A.M. & OWEN, R.M. (1991): The europium anomaly of seawater: implications for fluvial versus hydrothermal REE inputs to the oceans.– Chem. Geol., 92, 317–328.

PALINKAŠ, A.L. (1988): Geokemijske karakteristike paleozojskih metalogenetskih područja: Samoborska gora, Gorski Kotar, Lika, Kordun i Banija [*Geochemical characteristics of Paleozoic metallogenic regions: Samoborska gora, Gorski Kotar, Lika, Kordun and Banija* – in Croatian with English summary].– Unpubl. PhD Theses, University of Zagreb, 108 p.

PALINKAŠ, A.L. (1990): Siderite-barite-polysulfide and early continental rifting in Dinarides.– Geol. vjesnik, 43, 181–185.

PALINKAŠ, A.L., BOROJEVIĆ, S., STRMIĆ, S., PROCHASKA, W., SPANGENBERG, J.E. (2003): Siderite-hematite-barite-polysulfide mineral deposits, related to the Early intra-continental Tethyan rifting, Inner Dinarides.– In: ELIOPOULOS et al. (eds.): Mineral Exploration and Sustainable Development, Millpress, Rotterdam, 1221–1224.

PODUBSKI, V. (1969): Litostratigrafski razvitak paleozoika u sjeverozapadnoj Bosni [*Lithostratigraphic development of Palaeozoic in NW Bosnia* – in Serbian].– Geol. glasnik, 12, Sarajevo, 165–195.

SCHWIN, G. & MARKL, G. (2005): REE systematics in hydrothermal fluorite.– Chem. Geol., 216, 225–248.

STRMIĆ PALINKAŠ, S., SPANGENBERG, J.E. & PALINKAŠ, A.L. (2009): Organic and inorganic geochemistry of Ljubija siderite deposits, NW Bosnia and Herzegovina.– Miner. Deposita, 44/8, 893–913.

SUN, S.S. & MCDONOUGH, W.F. (1989): Chemical and isotopic systematics of oceanic basalts: implications for mantle composition and processes.– In: Magmatism in the ocean basins, Geological Society, Special Publication, 42, 313–345.

ŠARAC, M. (1981): Metalogenetske karakteristike rudnosneoblasti Ljubije [*Metallogenic chara-cteristics of the Ljubija ore-bearing area – in Serbian*].– Unpubl. PhD Theses, University of Belgrade, 135 p.

ŠARAC, M. & VITALJIĆ, B. (1973): Omarska – povećani sirovinski potencijal, Rudarsko–metalurškog kombinata "Zenica" [*Omarska – increased raw material potential of the ore and metallurgical combine "Zenica"* – in Serbian].– Čelik, 45, Zenica, 17–21.

TAYLOR, S.R. & McLENNAN, S.M. (1985): The continental crust: its composition and evolution.– Blackwell, Oxford, U.K., 312 p.

WINCHESTER, J.A. & FLOYD, P.A. (1977): Geochemical discrimination of different magma series and their differentiation products using immobile elements.– Chem. Geol., 20, 325–343.